Talanta 121 (2014) 1–8

Contents lists available at ScienceDirect

Talanta

journal homepage: www.elsevier.com/locate/talanta

Electro-oxidation and voltammetric determination of oxymetholone in the presence of mestanolone using glassy carbon electrode modified with carbon nanotubes

Abbas Afkhami *, Hamed Ghaedi, Tayyebeh Madrakian, Davood Nematollahi, Banafsheh Mokhtari

Faculty of Chemistry, Bu-Ali Sina University, Hamedan, Iran

ARTICLE INFO

Article history:
Received 4 June 2013
Received in revised form
12 December 2013
Accepted 23 December 2013
Available online 30 December 2013

Keywords:
Determination of oxymetholone
Electrochemical sensor
Square wave stripping voltammetry
Plasma sample
Pharmaceutical preparations

ABSTRACT

A new chemically modified electrode was constructed and applied to the electro-oxidation of the oxymetholone. Also, the electrode was applied to the simple, rapid, highly selective and sensitive determination of oxymetholone (OXM) in pharmaceutical and plasma samples using square wave voltammetry (SWV). The multi-walled carbon nanotubes modified glassy carbon electrode (MWCNT/GCE) were prepared by casting of the multi-walled carbon nanotubes (MWCNT) suspension on the glassy carbon electrode surface. The limit of detection and the linear range were found to be 1.36 and 2.00–90.00 ng mL^{-1} of OXM, respectively. The effects of potentially interfering substances on the determination of this compound were investigated and found that the electrode is highly selective. The proposed modified electrode was used for the determination of OXM in human plasma and pharmaceutical samples. This reveals that MWCNT/GCE shows excellent analytical performance for the determination of OXM in terms of very low detection limit, high sensitivity, very good repeatability and reproducibility over other methods reported in literature.

1. Introduction

Oxymetholone (OXM), 17-hydroxy-2-[hydroxymethylenel-17-methyl-5a-androstim-3-one, is an orally active 17a-alkylated anabolic–androgenic steroid first described by Ringold et a1. [1]. It has a fully saturated A-ring structure, which may reduce the risk of hepatotoxicity [2]. It is used in treating anemia. Clinical assessments of OXM have been made to establish the degree of anabolism and androgenicity of this steroid [3] and information on its side effects have been documented [3–5]. Despite the wide use of this steroid in pharmaceutical preparations and significant studies on side effects [4], relatively little is known about the solution chemistry of this compound. OXM [5] is a l,3-dicarbonyl compound, which can exist in three tautomeric forms I–III (Fig. 1) [6]. There is no quantitative information available regarding the positions of these equilibria and on solvent effects on them. Nevertheless, the structure of OXM is usually presented as I, which in nonhydroxylic media is stabilized by formation of an intramolecular hydrogen bond (IV). In hydroxylic solvents it is able to form intermolecular hydrogen bonds, the role of intramolecular hydrogen bonds is usually negligible whereas covalent solvation, resulting in formation of hydrates and hemiacetals, may occur in nonhydroxylic solvents. As aldehydes form hydrates and hemiacetals more readily than ketones [7], nucleophilic addition of the solvent will favor the formyl groups in structures II and III. As conjugation deactivates the carbonyl function toward hydrate and hemiacetal formation [7], stronger hydration and reaction with alcohols is predicted to involve structure II rather than III. In this structure, the presence of the electron-withdrawing carbonyl groups in the α-position can be expected to enhance the reactivity of the formyl group toward nucleophilic addition [6,7].

OXM is also used as a doping agent [8,9]. Intramuscular or deep subcutaneous injection is the principal route of administration of all anabolic steroids except the 17-alpha-substituted steroids as OXM, which are active, orally [10]. This is feasible because substitution at the 17-carbon protects the compound from the hepatic metabolism [11]. Many side-effects have reportedly been associated with chronic use of high doses of all oral anabolic–androgenic hormones including OXM. These include high blood pressure, water retention, prostate gland enlargement, gynecomastia (abnormal breast tissue growth in males) and liver damage. OXM is the anabolic steroid most associated with premature hair loss [8–11]. Consequently, the development of rapid, simple and accurate method with high sensitivity for the determination of

* Corresponding author. Tel./fax: +98 811 8272404.
E-mail address: afkhami@basu.ac.ir (A. Afkhami).

0039-9140/$ - see front matter © 2013 Elsevier B.V. All rights reserved.
http://dx.doi.org/10.1016/j.talanta.2013.12.047

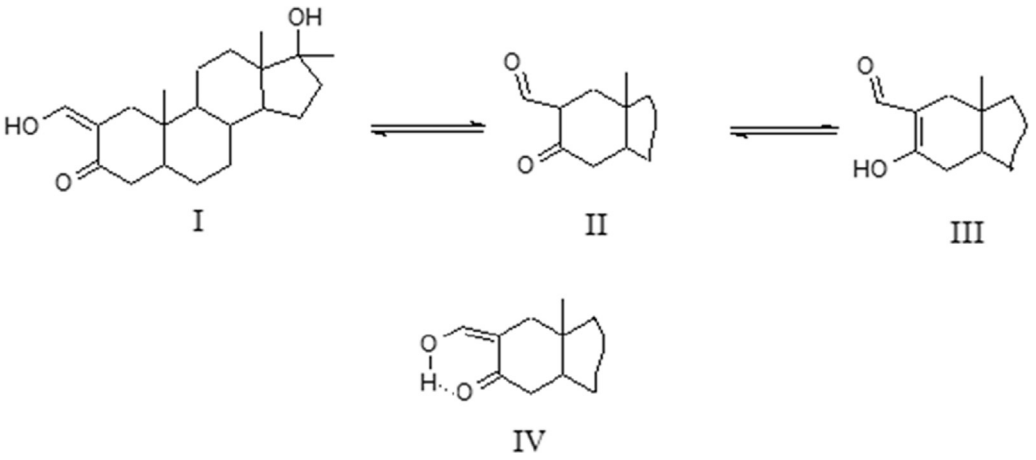

Fig. 1. Different tautomeric forms of OXM [7].

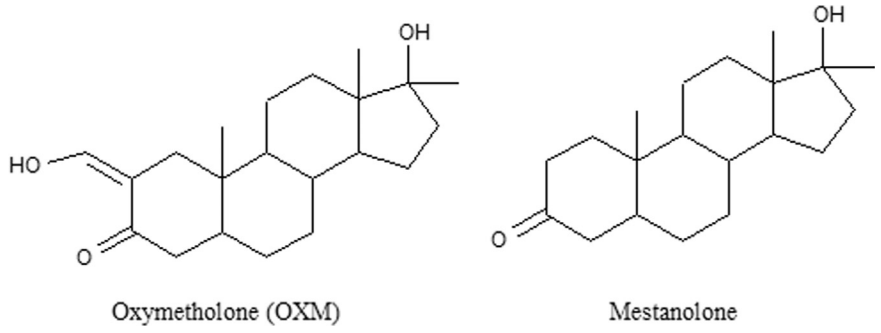

Fig. 2. Structures of OXM and mestanolone.

OXM at (ultra)trace levels in pharmaceutical and biological samples is of particular significance. To the best of our knowledge, there is no report on the determination of OXM by electrochemical methods. This shows the importance of the development of rapid, simple, sensitive and accurate electrochemical methods for measuring OXM.

The development of electrochemical sensors has been widely researched as an inexpensive method to sensitively detect a variety of biological analytes. Carbon based electrodes have been commonly used because of their low cost, good electron transfer kinetics and biocompatibility. Recently, carbon nanotubes (CNTs) have also been incorporated into electrochemical sensors. While they have many of the same properties as other types of carbon, CNTs offer unique advantages including enhanced electronic properties, a large edge plane/basal plane ratio, and rapid electrode kinetics [12].

To find new electrocatalytic surfaces, a suitable electrode substrate, such as glassy carbon (GC) or gold, is modified with a film or layer of CNTs. Several methods have achieved the electroanalysis of different analytes by using CNT modified electrodes. Benefits of low detection limits, increased sensitivity, decreased overpotentials and resistance to surface fouling are found by these CNTs-based electrodes [13]. Electrochemistry implies the transfer of charge from one electrode to another. Due to the curvature of the carbon graphene sheet in nanotubes, the electron clouds change from a uniform distribution around the C−C backbone in graphite to an asymmetric distribution inside and outside the cylindrical sheets of the nanotube [14]. Because the electron clouds are distorted, a rich π-electron conjugation forms outside the tube, therefore, making CNTs electrochemically active [14].

There are numerous reports of CNT-modified electrodes for the detection of different analytes with low detection limits, decreased overpotentials, and resistance to surface fouling [15–18].Therefore, CNT-based sensors generally have higher sensitivities, lower limits of detection, and faster electron transfer kinetics than traditional carbon electrodes. Many variables need to be tested and then optimized to create a CNT-based sensor. Electrode performance can depend on the synthesis method of the nanotube, CNT surface modification, the method of electrode attachment, and the addition of electron mediators [12].

The physical and catalytic properties make CNTs ideal for use in sensors. Most notably, CNTs display high electrical conductivity, chemical stability, and mechanical strength. The two main types of CNTs are single-walled CNTs (SWCNTs) and multi-walled carbon nanotubes (MWCNTs). SWCNTs are sp^2 hybridized carbon in a hexagonal honeycomb structure that is rolled into hollow tube morphology [19]. MWCNTs are multiple concentric tubes encircling one another [20].

In this work, a modified glassy carbon electrode was used as the working electrode for investigation of electro-oxidation behavior of OXM and determination of this anabolic steroid in the presence of its main metabolite mestanolone (Fig. 2) that its chemical structure is very similar to OXM, in the biological and pharmaceutical samples. To the best of our knowledge, this is the first report on the investigation of the oxidation and determination of OXM with the carbon electrode.

2. Experimental

2.1. Apparatus and chemicals

All electrochemical experiments including cyclic voltammetry (CV), square wave voltammetry (SWV) and impedance spectroscopy

were performed using an Autolab PGSTAT Model 302 N Potentiostat/Galvanostat connected to a three-electrode cell. It was controlled by a computer using Nova version 1.7 software. A conventional three-electrode system was used with a glassy carbon (GC) working electrode (unmodified or modified), a saturated Ag/AgCl reference electrode and a Pt wire as the counter electrode. A magnetic stirrer (PAR-305) with a Teflon-coated magnet was used to provide the convective transport during the preconcentration step. The whole measurements were automated and controlled through the programming capacity of the apparatus. The system was run on a PC using Nova 1.7 software. For impedance measurements, a frequency range from 100 kHz to 1.0 Hz was employed. The AC voltage amplitude was 5 mV, and the equilibrium time was 10 min. A Metrohm pH-meter, Model 713, with a combined glass electrode (Metrohm, Swiss), was used to determine pH values of the solutions.

All the chemicals were of analytical grade or better and used as received. Unless otherwise stated, all the solutions were prepared with doubly distilled water (DDW). Multi-walled carbon nanotubes (MWCNTs) (purity more than 95%) with outer diameter between 5 and 20 nm, inner diameter between 2 and 6 nm and tube length from 1 to 10 μm was from Plasmachem GmbH (Germany). Britton–Robinson (B–R) buffer was prepared in doubly distilled water (DDW) and was used as the supporting electrolyte. pH adjustments were performed with 0.01–1.0 mol L^{-1} HCl or NaOH solutions. Scanning electron microscopy (SEM) images were determined with an XL-30 ESEM (Philips, Netherland), and a glassy carbon wafer was used for SEM measurements.

2.2. Modification of the electrodes

For the pretreatment and activation of MWCNTs, 80 mg of carbon nanotubes were dispersed in 60 mL of 4.0 mol L^{-1} HNO_3 and heated for 24 h at 60 °C, then washed with DDW to neutrality and dried in an oven at 37 °C.

The GC electrode was polished to a mirror finish with alumina slurry (0.3 μm), and then was dipped into acetone for about 1 min, and sonicated in distilled water and ethanol (50:50) for a few minutes. MWCNTs were dispersed ultrasonically in the acetonitile solution to form a 0.4 mg mL^{-1} MWCNTs suspension. Then, 20 μL of the black solution was cast at the GC electrode surface and the solvent was evaporated at room temperature to prepare the MWCNTs/GC modified electrode. The electrode was then conditioned by potential cycling in the limited range of 0.000–0.500 V vs. Ag/AgCl in B – R buffer solution, as supporting electrolyte, until a steady state voltammogram was obtained. The prepared modified MWCNTs/GCE was used for the study of the electro-oxidation and electrochemical determination of OXM.

2.3. Experimental procedure

For voltammetric analysis of OXM, appropriate quantities of the analyte solution were placed in a 25 mL standard volumetric flask and diluted to the mark with a pH 5.0 (0.05 mol L^{-1}) B – R buffer and ethanol (75:25). The solution was then transferred into the electrochemical cell where the measurements were carried out. The voltammograms were recorded by scanning the potential towards the positive direction from +0.500 to +1.200 V vs. saturated Ag/AgCl. When necessary, renewal of the electrode surface was easily accomplished by soaking the modified electrode into the supporting electrolyte and cycling the potential between +0.400 V and +1.300 V vs. Ag/AgCl in pH 5.0 B – R buffer solutions twenty times before use so as to renew the electrode surface.

2.4. Analysis of plasma sample

OXM was determined after addition to human blood. Drug free human blood, obtained from healthy volunteers was centrifuged (3000 rpm) for 30 min at room temperature and separated serum samples were stored frozen until assay. Acetonitrile removes serum proteins more effectively, the addition of 1–1.5 vol of acetonitrile in serum is sufficient to remove the proteins. After vortexing for 30 s, the mixture was then centrifuged for 10 min at 3000 rpm to separate serum protein residues and the supernatant was taken carefully and used for the analysis by the proposed electrode.

2.5. Stability studies

Stability of OXM in plasma was studied at room temperature and at −20 °C. Control human plasma samples were spiked with 15 and 25 ng mL^{-1} of OXM. The short-term stability in plasma was measured at room temperature over the period required to process a batch of study samples. The long-term stability of OXM in frozen human plasma (−20 °C) was investigated at 24, 48, 72 h and 1, 2, 4, and 8 weeks. Samples were studied immediately after preparation as reference values and after storage. Prior to their analyses, samples were brought to room temperature and vortex-mixed well.

2.6. Pharmaceutical sample preparation

Ten pieces of OXM containing tablets i.e. Anadrol 50 (Alhavi Pharmaceutical Co., Tehran, Iran) were weighed and ground to a homogeneous powder in a mortar. A portion equivalent to a stock solution of a concentration of about 500 ng mL^{-1} was accurately weighed and transferred into a 10 mL volumetric flask and diluted to the volume with DDW. The contents of the flask were sonicated for 10 min to affect complete dissolution. Appropriate solutions were prepared by taking suitable aliquots of the clear supernatant liquid and diluting them with the B–R buffer solution of pH 5. Each solution was transferred into the voltammetric cell and analyzed by standard addition method. The square wave voltammograms were recorded between 0.400 and 0.950 V vs. Ag/AgCl after open-circuit accumulation for 130 s with stirring. The oxidation peak current of OXM was measured.

3. Results and discussion

3.1. Electrochemical characterization of the MWCNTs/GCE

Cyclic voltammetry (CV) was used to characterize the MWCNTs/GCE. Cyclic voltammograms for 1.0 mmol L^{-1} $Fe(CN)_6^{3-/4-}$ in 0.1 mol L^{-1} KCl solution on unmodified GCE and MWCNT/GC are shown in Fig. 3. The quasi-reversible one-electron redox behavior of ferricyanide ions was observed on the bare GCE with a peak separation (ΔE_p) of 0.240 V at the scan rate of 80 mV s^{-1}. After being modified with MWCNTs, the peak currents of $Fe(CN)_6^{3-/4-}$ increased, while the ΔE_p decreased (ΔE_p=0.200 V) compared with that observed at the bare GCE indicating that modification of surface electrode causes the charge transfer at the surface electrode was easier and faster.

The area of the electrode was obtained by the cyclic voltammetric method for 1.0 mmol L^{-1} $K_3Fe(CN)_6$ at different scan rates using Randles–Sevcik formula [21]. The area was found to be 1.64×10^{-2} cm^2 and 2.0×10^{-2} cm^2 for unmodified and modified electrodes, respectively.

In another attempt to clarify the differences among the electrochemical performance of the bare GCE and MWCNTs/GCE,

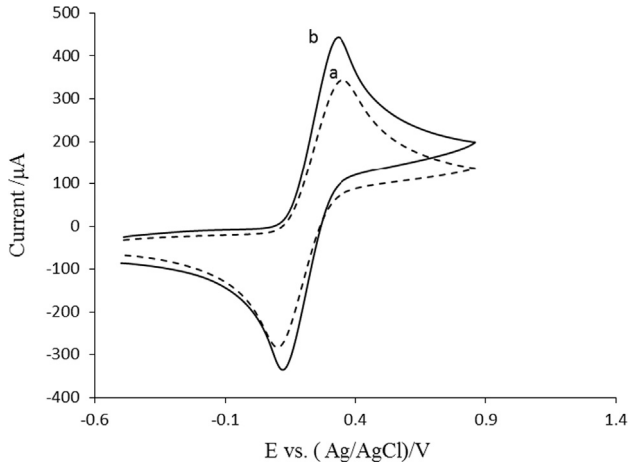

Fig. 3. Cyclic voltammograms for 1.0×10^{-3} mol L^{-1} $K_3[Fe(CN)_6]$ in 1.0 mol L^{-1} KCl obtained at GCE (a) and MWCNs/GCE (b); scan rate 80 mV s^{-1}.

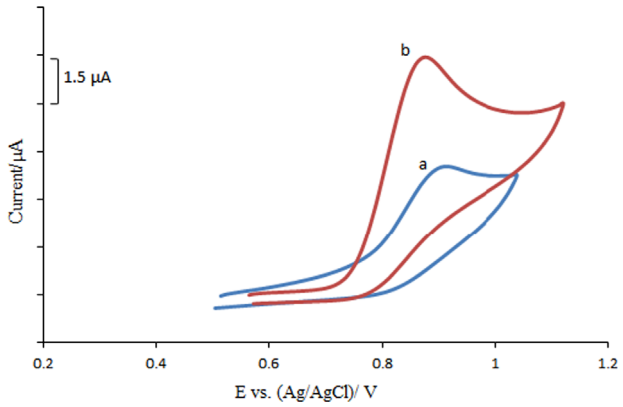

Fig. 4. Cyclic voltammograms of 35 ng mL^{-1} oxymethalone solution in B–R buffer of pH 5.0 obtained at (a) unmodified and (b) modified GCE. Condition: scan rate, 100 mV s^{-1}; accumulation time, 130 s.

electrochemical impedance spectroscopy (EIS) was used as a procedure for the characterization of each electrode surface. As such, the Nyquist plots for 1.0×10^{-3} mol L^{-1} $K_3[Fe(CN)_6]$ in 1.0 mol L^{-1} KNO_3 showed a significant difference in responses for the electrodes (Fig. S1). The semicircular elements correspond to the charge transfer resistances (R_{ct}) at the electrode surface with a large diameter, was observed for the bare GCE in the frequency range 10^{-1}–10^{6} Hz. However, the diameter of the semicircle diminished when modified GCE was employed. Additionally, the charge transfer resistance (R_{ct}) values obtained from this observation implied that the charge transfer resistance of the electrode surface decreased and the charge transfer rate increased upon using modified GCE. A Warburg at 45° was also observed for two electrodes of interest. The R_{ct} value for the modified GCE was smaller than that for bare GCE. Comparison of the R_{ct} obtained for the electrodes indicates that the modification of electrodes with MWCNTs caused easier and faster charge transfer at the electrode surface.

Also, SEM was employed to investigate the surface morphology of the MWCNTs/GCE as shown in Fig. S2. As seen in Fig. S2 it is clear that the GCE surface is coated with a homogeneous layer of MWCNTs.

3.2. Cyclic voltammetric behavior of OXM

The electrochemical behavior of OXM at the GCE and also at the MWCNT/GCE was studied by cyclic voltammetry at pH 5.0. The cyclic voltammograms obtained for 35.0 ng mL^{-1} OXM solution at a scan rate of 100 mV s^{-1} showed only one well-defined anodic peak in the potential range from 0.400 to 1.000 V vs. Ag/AgCl at MWCNs/GCE. The results are shown in Fig. 4. As seen, on the reverse scan, no corresponding reduction peak was detected showing that, the electrode process of OXM is an irreversible reaction (in this condition). The CV of OXM displayed a broad (S-shape) oxidation peak at about 0.900 V vs. Ag/AgCl at the bare GCE, while at the MWCNTs/GCE, a well-defined and sharp peak was obtained at about 0.860 V vs. Ag/AgCl which shows a negative shift of 40 mV. This indicates the effect of the modification by MWCNTs. On the other hand, the peak current of the OXM oxidation at the MWCNTs/GCE increased as compared to that at the GCE, which can be related to the high surface area of MWCNTs. These phenomena confirmed that the MWCNTs can efficiently accelerate the electron-transfer at the electrode surface and improve the electrochemical performance consequently.

On the other hand, it was found that the oxidation peak current of OXM showed a significant decrease during the successive cyclic voltammetric scans. After the second sweep, the peak current decreased greatly and finally remained unchanged. This phenomenon may be due to the adsorption of OXM or its oxidative product at the electrode surface and blocking of the electrode. Therefore, the voltammograms corresponding to the first cycle was generally recorded.

3.3. Influence of scan rate

To understand the reaction mechanism, the effect of scan rate on the peak currents of OXM at the MWCNTs/GCE at different scan rates from 20 to 260 mV s^{-1} was investigated. The oxidation peak current of OXM was linearly proportional with the scan rate in the range 20–260 mV s^{-1} in the B–R buffer solution of pH 5.0, with the equation of I_{pa} (μA)=0.1482υ (mV s^{-1})+0.7136 (r^2=0.9981). This indicates that the electrode process was controlled by adsorption rather than diffusion. A plot of logarithm of anodic peak current vs. logarithm of scan rate obtained a straight line with a slope of 0.9104 close to the theoretical value of 1.0, which is expected for an ideal reaction for the adsorption-controlled electrode process [22–25].

The E_p of the oxidation peak was dependent on the scan rate. The plot of E_p vs. log υ was linear. The relation between peak potential and log υ can be communicated by the equation, E_p=0.0545 log υ+0.86740 (0.9966), where E_p and υ are peak potential in V and scan rate in V s^{-1}, respectively. For an adsorption-controlled and irreversible electrode process, according to Laviron [23], E_p is defined by the following equation:

$$E_p = E^{o'} + \frac{2.303RT}{\alpha nF}\log\frac{RTk^0}{\alpha nF} + \frac{2.303RT}{\alpha nF}\log\upsilon$$

where α is the transfer coefficient, k_0 is the standard heterogeneous rate constant of the reaction, n is the number of electrons transferred, υ is the scan rate and $E^{o'}$ is the formal redox potential. Other symbols have their common meanings. Thus, the value of αn can be easily calculated from the slope of E_p vs. log υ. In this system, the slope was found to be 0.0545, taking T=298 K and substituting the values of R and F, αn was calculated to be 1.085.

Also, potentiostatic coulometry was applied in an alcoholic aqueous solution (buffer:ethanol (75:25)) containing 0.18 mmol of OXM at 0.80 V vs. Ag/AgCl. The electrolysis progress was monitored using cyclic voltammetry. It was found that, proportional to the advancement of coulometry, the anodic peak decreased. The anodic peak disappeared when the charge consumption was about $2e^-$ ($2.07\approx2$) per molecule of OXM. Therefore, α in the electrooxidation of OXM at MWCNT/GCE was calculated to be 0.54.

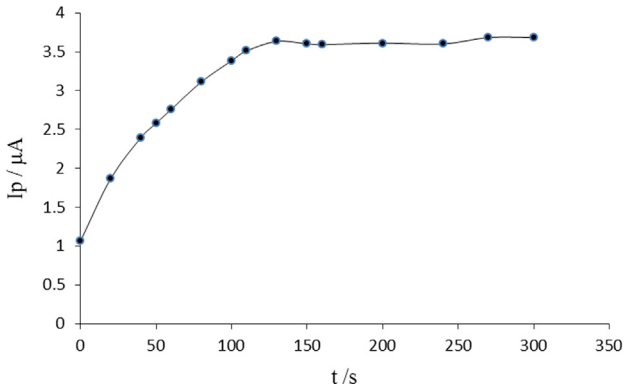

Fig. 5. Effect of accumulation time on the peak current (I_p/μA). Condition: scan rate, 100 mV s^{-1}; pH=5 and OXM concentration of 30 ng mL^{-1}.

3.4. Influence of accumulation potential and accumulation time

It was significant to fix the accumulation potential and accumulation time when adsorption studies were assumed. Both conditions could affect the amount of adsorption of OXM at the electrode. Bearing this in mind, the effect of accumulation potential and time on peak current response was studied by CV. The concentration of OXM used was 30 ng mL^{-1}. When accumulation potential was varied from +0.600 to −0.600 V vs. Ag/AgCl and also at open circuit condition, the peak current changed a little. Hence, accumulation at open circuit was approved. Also the influence of accumulation time ranging from 0 to 300 s on the oxidation of OXM at MWCNT/GCE was investigated (Fig. 5). The peak current increased gradually as the accumulation time increased from 0 to 130 s. However, with further increasing accumulation time beyond 130 s, the peak current tends to be almost stable. Therefore, the optimal accumulation time of 130 s was employed in further investigates.

3.5. Effect of the amount of MWCNTs on the oxidation peaks of OXM

The amount of modifier can change the properties and functions of the electrode surface. Thus, the effect of the amount of MWCNTs as a modifier was studied by adding 5–25 μL of dispersed MWCNTs onto the GC electrode surface. It was observed that the oxidation peak current increased with increase in the amount of MWCNTs up to 15 μL and then saturation in the anodic peak current was happened. Therefore, 15 μL of MWCNTs was selected as the optimum amount for the preparation of the MWCNT/GCE.

3.6. Effect of pH

Standard solutions of OXM (25 ng mL^{-1}) were used to obtain the optimum pH of the supporting electrolyte. The influence of the pH on the oxidation peak current of OXM was studied in the pH range 2.0–10.0 using B–R buffer. The results are shown in Fig. 6. It was observed that as the pH was step by step increased, the anodic peak potential shifted to less positive values, proposing the involvement of protons in the reaction. A plot of E_p vs. pH (Fig. 6A) gave a straight line from pH 2–7 with a slope of −0.0613 V/pH, which is very close to the anticipated Nernstian value of 0.059 V for a two electron–two proton process. Another straight line with a slope of −0.027 V/pH was obtained from pH 7–10. This behavior is in agreement with a two electrons–one proton process. The pK_a of 6.78 for OXM was evaluated from the intersection of the two linear segments of E_p vs. pH plot in the 25:75 (v/v) mixture of ethanol:water. The pK_a for OXM in water is reported as 4.5 [26].This shows that, as it is expected, OXM in the ethanol:water mixture is a weaker acid than that in water.

Nevertheless, as can be seen in Fig. 6B, the peak current increased with pH in the range 2.0–5.0 and dramatically decreased at higher pHs. Also the peak shape at pHs higher than 7.0 changed to the S-shape. This may be due to the fact that the predominant form of OXM at alkaline pHs is the anionic form (deprotonated form). Also in the alkaline media α-position protons were deprotonated, therefore the solubility of OXM in the aqueous solution increased. According to the results (Section 3.3) the electrooxidation of the OXM is an adsorption-controlled process, therefore an increase in the solubility of the OXM causes a decrease in the adsorption of OXM at the electrode surface (by dissolution) and then the concentration of the OXM at the electrode surface decreases, therefore the peak current decreases. Also by increasing the solubility of OXM in the aqueous solution and consequently decreasing the adsorption of OXM at the electrode surface, the over voltage for the oxidation of OXM increased and therefore the peak shape was changed to S-shaped. Furthermore, with increasing pH of the solution, the peak current decreased and the peak shape was changed to S-shape, due to the desorption and dissolution of anionic forms of OXM. Above pH 5.0, the oxidation reaction is facile and thus sharp oxidation peak is observed.

This phenomenon was also observed in the SWV technique and the peak current (I_p) reached its maximum value at pH 5.0. Thus, this pH was employed for further studies.

3.7. Suggested mechanism

We may assume that the oxidation steps of OXM were located on the A-ring, with two electron oxidation process (as noted before, obtained from potentiostatic coulometry). This mechanism may be due to the fact that OXM is a l,3-dicarbonyl compound, which can exist in three tautomeric forms I–III [6]. As conjugation deactivates the carbonyl function toward hydrate and hemiacetal formation [7], stronger hydration and reaction with alcohols is predicted to involve structure II rather than III [5,6,27].

In this case the OXM is tautomerized and structure II is formed. As noted before, the oxidation occurs at the A-ring of OXM. Additionally in the A-ring, there are two appropriate oxidation positions (positions 1 and 2, Scheme 1). If the oxidation is performed in position 1, a conjugated double bond is created. On the other hand, if the oxidation process occurs in position 2, superconjugated double bond is formed. Additionally the hydrogen is reserved in the α-position in the C_1 is more acidic than that in C_2, because the H in the C_1 is in the α-position relative to the two carbonyl groups. Due to the formation of super-conjugated double bond on one hand, and easier deprotonating of C_1 than C_2 on the other hand, the oxidation at position 2 takes place easier than that at position 1. The cyclic voltammogram for mestanolone, as the main metabolite of OXM, was also obtained in the same condition as for OXM. The CV did not show any anodic peak for mestanolone. As seen in Fig. 1, the mestanolone structure is very similar to the OXM. So if oxidation had occurred at position 1, an anodic peak for mestanolone should also be observed. These observations show that, oxidation of OXM at position 2 is more probable than that at position 1. The FT-IR spectra for OXM and its oxidation product, after separation and purification, were also recorded. A comparison between two spectra shows an increase in the intensity of the absorption band at around 1715 cm^{-1} (assigned to C=O band) by oxidation of OXM. Therefore the mechanism for the oxidation of OXM can be suggested as in Scheme 1.

3.8. Other optimum conditions

The optimum conditions for the square wave voltammetric signal of OXM were established by measuring the current dependence on

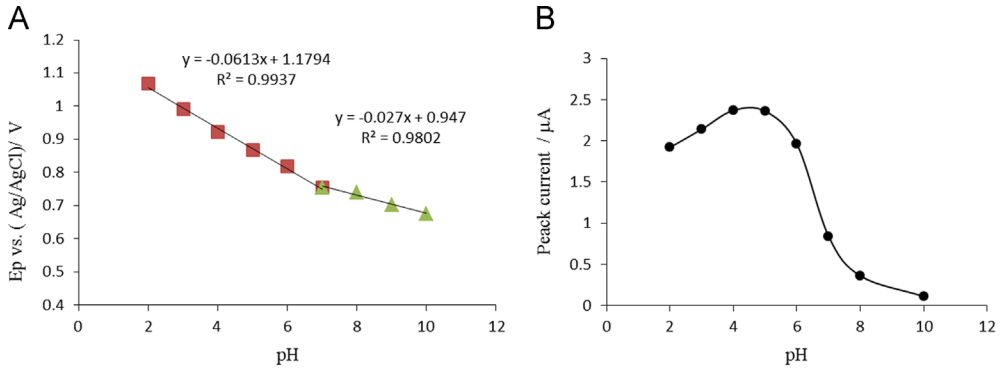

Fig. 6. Effect of pH on the E_p (A) and voltammetric response (B) for 25.0 ng mL^{-1} of OXM at MCNT/GCE. Condition: scan rate, 100 mV s^{-1}; deposition potential, open circuit; deposition time, 130 s; resting time, 10 s; SW frequency, 60 Hz; pulse amplitude, 90.0 mV.

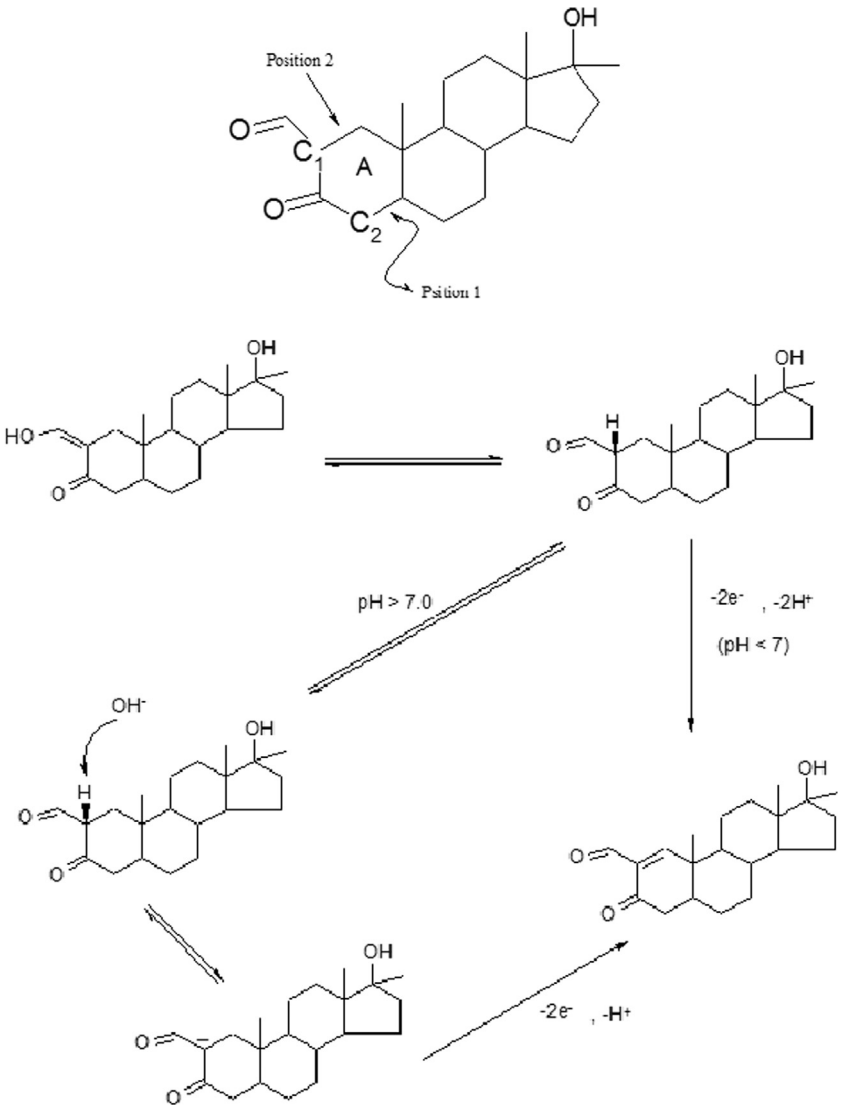

Scheme 1. The probable reaction mechanism for the oxidation of OXM at the surface of the modified electrode.

solution pH and some instrumental parameters including counting pulse amplitude, measuring time, pulse duration, and potential scan rate. These parameters were optimized for obtaining maximum signal to noise ratio. Optimum values for the studied parameters are given in Table 1.

3.9. Analytical characteristics

Under the optimized conditions described above, in order to obtain an analytical curve for the sensor, square wave voltammograms for oxidation of different concentrations of OXM^- were

Table 1
Optimum values for the studied parameters.

Parameter	Range studied	Optimum value
Accumulation potential (V vs. Ag/AgCl)	–0.600 to 0.600 and open circuit	Open circuit
Accumulation time (s)	0–300	130
Pulse amplitude (mV)	10–150	90
Voltage step (mV)	1–10	4.0
Frequency (Hz)	10–100	60

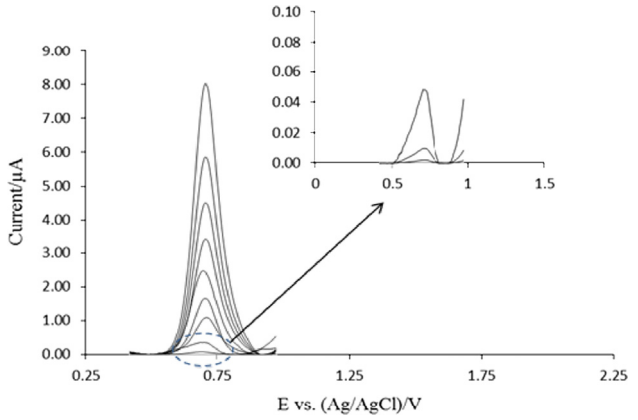

Fig. 7. Net square wave voltammograms for MWCNTs/GCE in the solutions with different concentrations of OXM. Conditions: pH, 5.0; deposition potential, open circuit; deposition time, 130 s; resting time, 10 s; SW frequency, 60 Hz; pulse amplitude, 90.0 mV.

carried out in B–R buffer solution of pH 5.0 (Fig. 7). The calibration graph was linear in the OXM concentration range 2.00–90.00 ng mL^{-1}. The calibration equation for OXM was, $I_{pa}=0.09C_{OXM}+0.0527$ ($R^2=0.9991$), where I_{pa} is the anodic peak current in μA and C_{OXM} is the concentration of OXM in ng mL^{-1}. A limit of detection of 1.36 ng mL^{-1} for OXM was obtained using a 3s/m ratio, where s is the standard deviation of the mean value for six SW voltammograms of the blank determined according to the IUPAC recommendations [27].

3.10. Interferences

In order to evaluate the selectivity of the method for the determination of OXM, the influence of potentially interfering substances on the determination of this compound was investigated. The tolerance limit for interfering species was considered as the maximum concentration that gave a relative error less than ±5.0% at a concentration of 10 ng $mL^{-1}$of OXM. No current response was observed for any of the studied compounds. Here one may note that the oxidation of biomolecules such as ascorbic acid, uric acid and citric acid often competes with that of OXM; however, the use of MWCNTs/GCE was successful to overcome this situation. Also, K^+, Ca^{2+}, NO_3^-, $NH4^+$ and Mg^{2+} have no effect on the I_p of OXM up to 120 fold excess. This suggests that the determination of OXM in the pharmaceutical and biological samples at MWCNTs/GCE is not affected significantly by the common interfering species present along with the molecules of interest. Additionally, the most important interference in the determination of any drug is its metabolites. Therefore, to study the effect of OXM metabolite on its determination by the proposed sensor, OXM was determined in the presence of mestanolone (Fig. 1), the major OXM metabolite [26]. The results showed that the metabolite did not interfere on the determination of OXM.

Table 2
Determination of OXM in spiked human plasma by the proposed method ($N=6$).

Spiked value (ng mL^{-1})	Found (ng mL^{-1})	Recovery (%)
–	0.0	–
5	4.9 ± 0.2	98.6
15	14.5 ± 0.8	96.9
60	61 ± 1	101.6

3.11. Analytical applications

The modified sensor was successfully applied to the determination of OXM in human plasma and tablet samples. OXM was determined after addition to the plasma sample and recovery values were calculated. The results are given in Table 2. The obtained recovery (between 96.9 and 101.6) and standard deviation values were acceptable. OXM in Anadrol 50 tablets (Inactive ingredients: lactose, magnesium stearate, povidone, starch) was determined using both the proposed and standard spectrophotometric [28] methods and the values of 48.9 ± 0.7 mg OXM $tablet^{-1}$ ($n=5$) and 49.3 ± 0.6 mg $tablet^{-1}$ ($n=5$) were obtained, respectively. For comparing the result of the suggested method with that of spectrophotometry, the student t-test was applied. The calculated value of t (1.28) for $P=0.05$ was smaller than the critical value ($t4=2.78$). Therefore, it can be concluded that there is no significant difference between the results obtained by the two methods for $P=0.05$.The satisfactory recovery of OXM in human plasma and the good agreement between the obtained value with that obtained by the standard method for tablet sample indicate that the proposed method has great potential in the practical sample analysis. Thus the sensor provides a good alternative for the determination of OXM in real samples.

3.12. Stability studies

Stability of OXM in human plasma was investigated under different conditions at 15.0 and 25.0 ng mL^{-1} concentrations and compared with data obtained from freshly prepared samples. OXM was stable in plasma for at least 4 h at room temperature (25 °C), period required to process a batch of study samples. The respective mean recoveries at 15.0 and 25.0 ng mL^{-1} were 96.80% and 93.60%, respectively. The compound was also stable in human plasma when stored at −20 °C for at least two weeks. The recoveries for 15.0 and 25.0 ng mL^{-1} were 98.15% and 102.10%, respectively.

3.13. Repeatability and reproducibility of the MWCNTs/GCE

The repeatability of the electrode in the determination of OXM was evaluated by performing six determinations with the same standard solutions of OXM. The relative standard deviation (RSD) for the response of electrode towards a 15.0 and a 30.0 ng mL^{-1} solution was found to be 3.6% and 2.2%, respectively. The reproducibility of the response of electrode was also studied. Six electrodes were prepared from the same batch and were evaluated by performing the determination of 30.0 ng mL^{-1} of OXM solution. The RSD for the response of between electrodes was 2.4%. The results show that the repeatability and reproducibility of the sensor for the determination of OXM are acceptable.

The modified electrode was stable up to five days. After five days the modified layer of MWCNTs began to destroy and swell and it was completely destroyed after 8 days.

4. Conclusion

The proposed method proved to be useful and reliable for the determination of OXM in human plasma and pharmaceutical samples. The sensitivity was enhanced considerably by preconcentration of OXM at the modified electrode surface and also due to the presence of MWCNTs. Moreover, the proposed method is very sensitive having sub-microgram detection limit for the determination of OXM. Finally, the sensor was applied to the determination of OXM in human plasma and pharmaceutical samples and the results are satisfactory, which suggests that MWCNTs/GCE can act as a powerful sensor for the determination of OXM in biological and pharmaceutical samples. To the best of our knowledge, this is the first report on the study of electro-oxidation and determination of OXM with the carbon electrode. The results revealed that MWCNTs/GCE shows excellent analytical performance for the determination of OXM in terms of very low detection limit, high sensitivity, very good repeatability and reproducibility.

Acknowledgments

The authors acknowledge the Bu-Ali Sina University Research Council and Center of Excellence in Development of Environmentally Friendly Methods for Chemical Synthesis (CEDEFMCS) for providing support to this work.

Appendix A. Supplementary material

Supplementary data associated with this article can be found in the online version at http://dx.doi.org/10.1016/j.talanta.2013.12.047.

References

[1] H.J. Ringold, E. Batres, O. Halpern, E. Necoechea, J. Am. Chem. Soc. 81 (1959) 427–432.
[2] H.D. Lennon, Steroids 7 (1966) 157–170.
[3] W. Martindale, in: A. Wade, E. F. J. Reynolds (Eds.), The Extra Pharmacopoeia, 27th ed., The Pharmaceutical Press, 1 Lambeth High Street, London.
[4] D.K. Keele, J.W. Worley, Am. J. Dis. Child. 113 (1967) 422–430.
[5] Merck Index; 9th ed., Merck: Rahway, NJ, 1976, p. 902.
[6] A.M. Bond, D. Dakternieks, P.P. Deprez, P. Zuman, J. Org. Chem. 53 (1988) 1991–1996.
[7] F.A.J. Meskens, Synthesis (1981) 501–522.
[8] International Olympic Committee, List of Classes of Prohibited Substances and Methods of Doping, IOC, Lausanne, 2001.
[9] W. Schänzer, Clin. Chem. 42 (1996) 1001–1020.
[10] J.D. Wilson, Androgens, in: J.G. Hardman, et al., (Eds.), Gilman's The Pharmacologic Basis of Therapeutics, 9th ed.,McGraw-Hill, New York, 1996.
[11] US Department of Health and Human Services, Toxicology and Carcinogenesis Studies of Oxymetholone, 2013, Text online at ⟨http://toxnet.nlm.nih.gov/cgi-bin/sis/search/a?dbs+hsdb:@term+@DOCNO+3374⟩ (accessed 25 April 2013).
[12] C.B. Jacobs, M.J. Peairs, B.J. Venton, Anal. Chim. Acta 662 (2010) 105–127.
[13] J. Wang, Electroanalysis 17 (2005) 7–14.
[14] J. Li, in: M. Meyyappan (Ed.), Carbon Nanotube Applications: Chemical and Physical Sensors, in Carbon Nanotubes Science and Application, CRC Press, New York, 2005, pp. 213–233.
[15] S. Timur, U. Anik, D. Odaci, L. Gorton, Electrochem. Commun. 9 (2007) 1810–1815.
[16] P. Arias, N.F. Ferreyra, G.A. Rivas, S. Bollo, J. Electroanal. Chem. 634 (2009) 123–126.
[17] D. Odaci, A. Telefoncu, S. Timur, Sens. Actuators B 132 (2008) 159–165.
[18] A. Arvinte, A.C. Westermann, A.M. Sesay, V. Virtanen, Sens. Actuators B 150 (2010) 756–763.
[19] S. Iijima, T. Ichihashi, Nature 363 (1993) 603–605.
[20] S. Iijima, Nature 354 (1991) 56–58.
[21] A. Sevcik, Coll. Czech. Chem. Commun. 13 (1948) 349–377.
[22] D.K. Gosser, Cyclic Voltammetry: Simulation and Analysis of Reaction Mechanisms, VCH, New York, 1993, p. 43.
[23] E. Laviron, J. Electroanal. Chem. 101 (1979) 19–28.
[24] A.J. Bard, L.R. Faulkner, Electrochemical Methods Fundamentals and Application, 2nd ed., Wiley (2004) 236.
[25] G. Alberti, R. Palombari, F. Pierri, Solid State Ion. 97 (1997) 359–364.
[26] D.M. Smith, J.W. Steele, Can. J. Pharm. Sci. 16 (1981) 68–72.
[27] Analytical Methods Commitee, Analyst 112 (1987) 199–204.
[28] Oxymetholone Tablets, in Online British Pharmacopoeia, vol III, 2012. Available at ⟨http://bp2012.infostar.com.cn/Bp2012.aspx?a=query&title=%22Oxymetholone+Tablets%22&tab=a-z+index&l=O&xh=1⟩. (accessed December 11, 2013).